Journal of Photochemistry and Photobiology A: Chemistry 205 (2009) 12–18

Contents lists available at ScienceDirect

Journal of Photochemistry and Photobiology A: Chemistry

journal homepage: www.elsevier.com/locate/jphotochem

Synthesis, photophysics and photochemistry of novel *tetra*(quinoxalinyl)phthalocyaninato zinc(II) complexes

Ali Erdoğmuş[a,b], Abimbola Ogunsipe[a,c], Tebello Nyokong[a,*]

[a] Department of Chemistry, Rhodes University, Grahamstown 6140, South Africa
[b] Department of Chemistry, Yildiz Technical University, 34210 Esenler, Istanbul, Turkey
[c] Department of Chemistry, University of Lagos, Lagos, Nigeria

ARTICLE INFO

Article history:
Received 24 February 2009
Received in revised form 1 April 2009
Accepted 8 April 2009
Available online 18 April 2009

Keywords:
Phthalocyanine
Photodynamic therapy
Non-planar distortion
Quantum yield
Singlet oxygen
Quenching

ABSTRACT

The syntheses and spectral, photophysical and photochemical properties of some zinc phthalocyanine derivatives – {2, (3)-*tetra*(quinoxalinyl)phthalocyaninato zinc(II), (β-ZnPc) and 1, (4)-*tetra*(quinoxalinyl)phthalocyaninato zinc(II), (α-ZnPc)} – are presented. The β-substituted complex is more fluorescent and exhibits lower tendencies to undergo intersystem crossing than its α-substituted counterpart, as judged by the former's higher fluorescence quantum yield (Φ_F) and lower triplet quantum yield (Φ_T) than the latter's in three solvents (DMSO, DMF and toluene). Singlet oxygen quantum yield (Φ_Δ) values show the same trends as Φ_T values. The differences in the spectral and photophysical properties of α-ZnPc and β-ZnPc are partly attributed to greater molecular distortions in the former. Studies of the interaction of the triplet states of α-ZnPc and β-ZnPc with triplet oxygen showed that α-ZnPc is more vulnerable to oxygen quenching than β-ZnPc. Also, the smallest quenching rate constants were observed in DMSO, which is attributed to the higher viscosity of DMSO than DMF and toluene.

1. Introduction

Phthalocyanine (Pc) and its metal complexes (metallophthalocyanines, MPcs) possess an 18π-electron macrosystem and display unique optical and physicochemical properties, which explain the wide use of these compounds in modern science and technology. Pcs and MPcs have found relevance in a wide array of applications, which include: electrocatalysis [1,2], photocatalysis [3,4], non-linear optics [5,6], chemical sensors [7,8] and in photovoltaic cells [9]. Worth mentioning is their medical application, particularly in the photodynamic therapy (PDT) of cancer [10–15]. In order to exploit the applicability of Pcs and MPcs in PDT, a thorough photophysicochemical study on these compounds is essential. The chief cytotoxin in PDT is singlet oxygen, which is formed via energy transfer from the excited triplet state of the Pc or MPc (photosensitizer) to ground state molecular oxygen. The excited triplet state of the photosensitizer then becomes an imperative entity during photosensitization. Factors which populate the excited triplet state are desirable in PDT, and this makes an MPc a better candidate in this respect than a Pc, particularly when the metal is heavy or paramagnetic (considering spin–orbit coupling). However, MPcs with open-shell and paramagnetic metal ions suffer the setback of possessing relatively short triplet lifetimes [16,17], leaving MPcs with closed-shell diamagnetic and heavy metal ions, as the preferred candidates for PDT consideration. This work describes for the first time the synthesis and photophysical and photochemical properties of two quinoxalynol-substituted phthalocyanines, incorporating zinc(II) ions. The new complexes present a possibility of quaternization and hence water solubility.

The triplet states of photosensitizers are highly vulnerable to quenching by oxygen molecules in their vicinity. The ubiquity of oxygen necessitates the deaeration of solutions meant for triplet state measurements; hence inert gases such as nitrogen and argon are used to purge the solutions before commencement of measurements. The effect of oxygen on the rate of deactivation of the excited triplet states of these quinoxalinyl-derivatized MPcs is also investigated.

2. Experimental

2.1. Materials and equipment

Dimethyl sulfoxide (DMSO), *N*,*N*′-dimethylformamide (DMF), chloroform ($CHCl_3$), methanol, pentanol, n-hexane, acetone and toluene were purchased from SAARCHEM; chlorophyll a, zinc phthalocyanine (ZnPc) 1,2-diphenyl*iso*benzofuran (DPBF), 3-nitrophthalonitrile, 4-nitrophthalonitrile, 2-quinoxalinol, 1,8-

* Corresponding author at: Department of Chemistry, Rhodes University, P.O. Box 94, Grahamstown 6140, South Africa. Tel.: +27 46 6038260.
E-mail address: T.nyokong@ru.ac.za (T. Nyokong).

1010-6030/$ – see front matter © 2009 Elsevier B.V. All rights reserved.
doi:10.1016/j.jphotochem.2009.04.007

diazabicyclo[5.4.0] undec-7-ene (DBU), potassium carbonate and zinc acetate were purchased from Aldrich.

FT-IR spectra (KBr pellets) were recorded on a Perkin-Elmer spectrum 2000 FT-IR spectrometer. UV–vis spectra were recorded on a Cary 500 UV/Vis/NIR spectrophotometer. ^{1}H NMR spectra were obtained in DMSO-d_6 using a Bruker EMX 400 NMR spectrometer. Elemental analyses were done on Vario Elementar EL III. Fluorescence spectra were recorded on the Varian Eclipse spectrofluoremeter. Triplet absorption and decay kinetics were recorded on a laser flash photolysis system, the excitation pulses were produced by a Nd:YAG laser (Quanta-Ray, 1.5 J/90 ns) pumping a dye laser (Lambda Physic FL 3002, Pyridin 1 in methanol). The analyzing beam source was from a Thermo Oriel xenon arc lamp, and a photomultiplier tube was used as detector. Signals were recorded with a two-channel digital real-time oscilloscope (Tektronix TDS 360); the kinetic curves were averaged over 256 laser pulses. Photo-irradiations were done using a General electric Quartz line lamp (300 W). A 600 nm glass cutoff filter (Schott) and a water filter were used to filter off ultraviolet and infrared radiations respectively. An interference filter (Intor, 670 nm with a band width of 20 nm) was additionally placed in the light path before the sample. Light intensities were measured with a POWER MAX 5100 (Molelectron detector incorporated) power meter.

2.2. Synthesis

2.2.1. 3-(2-Quinoxalinyl)-phthalonitrile (**1**)

The 3-nitrophthalonitrile (4.60 g, 27 mmol) was dissolved in DMF (60 ml) under argon and 2-quinoxalinol (3.88 g, 27 mmol) was added. After stirring for 30 min at room temperature, finely ground anhydrous potassium carbonate (11 g, 81 mmol) was added in portions during 4 h with efficient stirring. The reaction mixture was stirred and monitored by thin layer chromatography (TLC) using $CHCl_3$, under argon atmosphere at room temperature for 48 h. Then the mixture was poured into 250 ml of iced water, and the precipitate was filtered off, washed with water and methanol and then dried. The residue was recrystallized from methanol. The yield was 2.75 g (38%). IR spectrum (cm^{-1}): 3068 (Ar–CH), 2234 (CN), 1597 (C=C), 1487, 1401, 1377, 1339, 1308, 1241, 1197, 1132, 1084 (C–O–C), 1018, 996, 948, 919, 863, 833, 767, 751, 704. ^{1}H NMR ($CDCl_3$): δ ppm = 8.85 (1H, s, Ar–H), 8.17 (d, J = 7.71 Hz, 1H, Ar–H), 7.95 (1H, s, Ar–H), 7.86 (d, J = 14.42 Hz, 1H, Ar–H), 7.74–7.65 (4H, m, Ar–H). Calcd for $C_{16}H_8N_4O$: C, 70.58; H, 2.96; N, 20.58%. Found: C, 70.56; H, 2.69; N, 20.61%.

2.2.2. 4-(2-Quinoxalinyl)-phthalonitrile (**2**)

The 4-nitrophthalonitrile (2.96 g 17.1 mmol) was dissolved in DMF (30 ml) under argon and 2-quinoxalinol (2.5 g 17.1 mmol) was added. After stirring for 30 min at 40 °C, finely ground anhydrous potassium carbonate (5.9 g 42.5 mmol) was added in portions during 4 h with efficient stirring. The reaction mixture was stirred and monitored by TLC ($CHCl_3$) under argon atmosphere at 40 °C for 48 h. Then the mixture was poured into 200 ml iced water, and the precipitate was filtered off, washed with water and methanol and then dried. The crude product was chromatographed over a silica gel column using a mixture of $CHCl_3$:MeOH (100/1 by volume) as eluent. Finally the pure product was dried in vacuum. The yield was 0.5 g (11%). IR spectrum (cm^{-1}): 3093 (Ar–CH), 2227 (C≡N), 1563 (C=C), 1504, 1464, 1406, 1379, 1340, 1300, 1258, 1203, 1174, 1136, 1088 (C–O–C), 1020, 1008, 960, 929, 808, 792, 776, 762, 740, 693. ^{1}H NMR ($CDCl_3$): δ = 8.77 (1H, s, Ar–H), 8.13 (d, J = 8.65 Hz, 1H, Ar–H), 7.84 (1H, s, Ar–H), 7.86 (d, J = 12.66 Hz, 1H, Ar–H), 7.78–7.59 (4H, m, Ar–H). Calcd for $C_{16}H_8N_4O$: C, 70.58; H, 2.96; N, 20.58%. Found: C, 70.52; H, 2.99; N, 20.34%.

2.2.3. 1, (4)-tetra(quinoxalinyl)phthalocyaninato zinc(II) (α-ZnPc)

Compound **1** (0.50 g, 1.84 mmol), anhydrous zinc acetate (0.4 g, 1.84 mmol) and 4 ml of dry pentanol were placed in a standard Schlenk tube in the presence of 1,8-diazabicyclo[5.4.0] undec-7-ene (DBU) (0.4 ml, 0.28 mmol) under a nitrogen atmosphere and held at reflux temperature for 12 h. After cooling to room temperature, the reaction mixture was precipitated by adding it drop-wise into n-hexane. The crude product was precipitated, collected by filtration and washed with n-hexane. The crude product was dissolved in DMF. After concentrating, the dark green product was precipitated with hot ethanol and washed with ethanol, acetone, chloroform, n-hexane and diethyl ether. Furthermore this product was purified with preparative thin layer chromatography (silica gel) using $CHCl_3$–MeOH (3:1) solvent system. The yield was 50 mg (12%). UV–vis (DMSO): λ_{max} nm ($\log\varepsilon$) 327 (4.58), 620 (4.33), 687 (5.07), (DMF): λ_{max} nm ($\log\varepsilon$) 325 (4.34), 617 (4.20), 685 (4.99), (toluene): λ_{max} nm ($\log\varepsilon$) 354 (4.21), 620 (3.99), 690 (4.61). IR spectrum (cm^{-1}): 3063 (Ar–CH), 1644, 1591 (C=C), 1569, 1465, 1395, 1337, 1300, 1266, 1217, 1120, 1084 (C–O–C), 1044, 995, 941, 919, 873, 827, 760, 747 (Pc skeletal). ^{1}H NMR ($CDCl_3$): δ = 8.51 (4H, s, Pc–H), 7.96 (d, J = 8.48 Hz, 4H, Pc–H), 7.72 (4H, s, Ar–H), 7.61 (d, J = 15.21 Hz, 4H, Pc–H), 7.45–7.20 (16H, m, Ar–H). Calcd for $C_{64}H_{32}N_{16}O_4Zn$: C, 66.58; H, 2.79; N, 19.41%. Found: C, 64.90; H, 2.64; N, 19.14%.

2.2.4. 2, (3)-tetra(quinoxalinyl)phthalocyaninato zinc(II) (β-ZnPc)

Compound **2** (0.30 g, 1.10 mmol), anhydrous zinc acetate (0.12 g, 0.55 mmol) and 2.5 ml of dry pentanol were placed in a standard Schlenk tube in the presence of 1,8-diazabicyclo[5.4.0] undec-7-ene (DBU) (0.2 ml, 0.14 mmol) under nitrogen atmosphere and held at reflux temperature for 8 h. After cooling to room temperature, the reaction mixture was precipitated by adding it drop-wise into n-hexane. After collecting by filtration, the green product was dissolved in chloroform and was precipitated with hot ethanol and washed with ethanol, acetone and hexane. For further purification, the crude green product was chromatographed over a silica gel column using a mixture of $CHCl_3$: MeOH (50/1 by volume) as eluent. The yield was 40 mg (10%). UV–vis (DMSO): λ_{max} nm ($\log\varepsilon$) 359 (4.14), 614 (3.81), 679 (4.48), (DMF): λ_{max} nm ($\log\varepsilon$) 348 (4.18), 609 (3.84), 676 (4.54), (toluene): λ_{max} nm ($\log\varepsilon$) 357 (3.97), 611 (3.65), 676 (4.23). IR spectrum (cm^{-1}): 3061 (Ar–CH), 1610, 1588 (C=C), 1568, 1484, 1398, 1334, 1299, 1265, 1228, 1200, 1127, 1088 (C–O–C), 1047, 1018, 998, 965, 919, 880, 814, 757, 741 (Pc skeletal). ^{1}H NMR ($CDCl_3$): δ = 8.31 (4H, s, Pc–H), 7.88 (d, J = 6.82 Hz, 4H, Pc–H), 7.62 (4H, s, Ar–H), 7.54 (d, J = 14.82 Hz, 4H, Pc–H), 7.36–7.12 (16 H, m, Ar–H). Calcd for $C_{64}H_{32}N_{16}O_4Zn$: C, 66.58; H, 2.79; N, 19.41%. Found: C, 65.49; H, 2.69; N, 19.22%.

2.3. Photophysical and photochemical studies

2.3.1. Fluorescence quantum yields and lifetimes

Fluorescence quantum yields (Φ_F) were determined by the comparative method) [18,19], (Eq. (1)):

$$\Phi_F = \Phi_{F(Std)} \frac{F \cdot A_{Std} \cdot n^2}{F_{Std} \cdot A \cdot n_{Std}^2} \quad (1)$$

where F and F_{Std} are the areas under the fluorescence curves of α- or β-ZnPc and the standard respectively. A and A_{Std} are the respective absorbances of the sample and standard at the excitation wavelengths (which was ~0.05 in all solvents used), and n and n_{Std} are the refractive indices of solvents used for the sample and standard respectively. Chlorophyll a in ether (Φ_F = 0.32) [20] was employed as the standard. Both the sample and standard were excited at the same wavelength (630 nm).

2.3.2. Triplet quantum yields and lifetimes

The solutions for triplet quantum yields and lifetimes were introduced into a 1.0 mm pathlength UV–visible spectrophotometric cell, deaerated using nitrogen and irradiated at the Q band maxima. Triplet state quantum yields (Φ_T) of α- and β-ZnPc were determined by the triplet absorption method [21], using zinc phthalocyanine (ZnPc) as a standard; Eq. (2):

$$\Phi_T = \Phi_T^{Std} \cdot \frac{\Delta A_T . \varepsilon_T^{Std}}{\Delta A_T^{Std} . \varepsilon_T} \quad (2)$$

where ΔA_T and ΔA_T^{Std} are the changes in the triplet state absorbances of α- or β-ZnPc and the standard respectively. ε_T and ε_T^{Std} are the triplet state molar extinction coefficients for α- or β-ZnPc and the standard respectively. Φ_T^{Std} is the triplet quantum yield for the standard, ZnPc (Φ_T = 0.65 in DMSO [22], 0.58 in DMF [23] and 0.65 in toluene [24]). ε_T and Φ_T^{Std} were determined from the molar extinction coefficients of their respective ground singlet state (ε_S and ε_S^{Std}) and the changes in absorbances of the ground singlet states (ΔA_S and ΔA_S^{Std}), according to Eq. (3):

$$\varepsilon_T = \varepsilon_S . \frac{\Delta A_T}{\Delta A_S} \quad (3)$$

Quantum yields of internal conversion (Φ_{IC}) were obtained from Eq. (4), which assumes that only three processes (fluorescence, intersystem crossing and internal conversion), jointly deactivate the excited singlet state of the α- or β-ZnPc molecule:

$$\Phi_{IC} = 1 - (\Phi_F + \Phi_T) \quad (4)$$

2.3.3. Singlet oxygen quantum yields

Quantum yields of singlet oxygen photogeneration were determined in air (no oxygen bubbled) using the relative method with ZnPc as reference and DPBF as chemical quencher for singlet oxygen, using Eq. (5):

$$\Phi_\Delta = \Phi_\Delta^{Std} \cdot \frac{R_{DPBF} I_{abs}^{Std}}{R_{DPBF}^{Std} I_{abs}} \quad (5)$$

where Φ_Δ^{Std} is the singlet oxygen quantum yield for the standard, ZnPc (Φ_Δ = 0.67 in DMSO [25], 0.56 in DMF [26], and 0.58 in toluene [27]). R_{DPBF} and R_{DPBF}^{Std} are the DPBF photobleaching rates in the presence of α- or β-ZnPc and the standard respectively. I_{abs} and I_{abs}^{Std} are the rates of light absorption by α- or β-ZnPc and the standard respectively. To avoid chain reactions induced by DPBF in the presence of singlet oxygen [26], the concentration of DPBF was $\sim 3 \times 10^{-5}$ mol L^{-1}. Solutions of sensitizer (absorbance = 0.2 at the irradiation wavelength) containing DPBF were prepared in the dark and irradiated in the Q band region using the setup described above. DPBF degradation at 417 nm was monitored. The light intensity for singlet oxygen studies was 2×10^{15} photons s^{-1} cm^{-2}. The error in the determination of Φ_Δ was ~10% (determined from several Φ_Δ values).

2.3.4. Photodegradation quantum yields

For determination of photodegradation quantum yields, the usual Eq. (6) was employed:

$$\Phi_{Pd} = \frac{(C_0 - C_t) V N_A}{I_{abs} S t} \quad (6)$$

where C_0 and C_t in mol dm^{-3} are the concentrations of α- or β-ZnPc before and after irradiation respectively; V is the reaction volume; S, the irradiated cell area (2.0 cm^2); t, the irradiation time; N_A, Avogadro's number and I_{abs}, the overlap integral of the radiation source intensity and the absorption of α- or β-ZnPc (the action spectrum) in the region of the interference filter transmittance. The light intensity for photodegradation studies was 5×10^{16} photons s^{-1} cm^{-2}.

3. Results and discussion

3.1. Syntheses and characterization

The synthetic routes to α-ZnPc and β-ZnPc are summarized in Scheme 1. The first step in the synthetic procedure was to obtain **1** and **2**. These reactions were accomplished by a base-catalysed nucleophilic aromatic nitro displacement [28] of 3- and 4-nitrophthalonitrile with 2-quinoxalinol. The compounds were characterized by IR, UV–vis, NMR spectroscopies, and elemental analysis. The characteristic vibrations corresponding to ethers groups (C–O–C) at ca. 1070–1090 cm^{-1} were observed for both complexes **1** and **2**. The ^{1}H NMR spectrum of **1** and **2** showed signals at δ ranging from 7.59 to 8.85, belonging to aromatic protons, integrating for 8 protons for **1** and **2** each as expected. The results of the elemental analysis confirmed the proposed structure of compounds **1** and **2**.

To obtain substituted phthalocyanines, generally substituted phthalonitriles or 1,3-diiminino-1 *H*-isoindoles are used. 2(3), 9(10), 16(17), 23(24)-tetra-substituted phthalocyanines can be synthesized from 4-substituted phthalonitriles while 1(4), 8(11), 15(18), 22(25)-tetra-substituted phthalocyanines are produced from 3-substituted phthalonitriles. In both cases a mixture of four possible structural isomers are obtained. These isomers can be designed by their molecular symmetry as D_{4h}, C_{2v}, C_s and D_{2h}. In this work, we obtained phthalocyanines as isomeric mixtures as expected. No attempt was made to separate the isomers of α-ZnPc and β-ZnPc [29].

The metallo-phthalocyanines α-ZnPc and β-ZnPc were synthesized from the corresponding substituted phthalonitriles and corresponding metal salt (Zn [30]) in pentanol reflux temperature for 8 or 12 h (Scheme 1). The FTIR spectrum of α-ZnPc and β-ZnPc clearly indicates the cyclotetramerization of compounds **1** and **2** with the disappearance of the CN peaks at 2227 and 2234 cm^{-1} [31,32]. The characteristic vibrations corresponding to ether groups (C–O–C) were observed at 1084 (for **1**) and 1088 cm^{-1} (for **2**) and aromatic C–H stretching at ca. 3060 for the ZnPc complexes. Both of ZnPc derivatives showed absorption peaks between 700 and 1000 cm^{-1}, which may be assigned to phthalocyanine skeletal vibrations [33].

The ^{1}H NMR spectra of tetra-substituted phthalocyanine derivatives (α-ZnPc and β-ZnPc) showed complex patterns due to the mixed isomer character of these compounds. The compounds were found to be pure by ^{1}H NMR with both the substituents and ring protons observed in their respective regions. In the ^{1}H NMR spectrum of α-ZnPc the aromatic and Pc protons appear between 7.20 and 8.51 ppm and for β-ZnPc between 7.12 and 8.31 ppm, integrating for a total of 32 for each complex. It has been reported before that for large Pc molecules as in this work, elemental analyses often gives unsatisfactory results [34]. With this in mind, the elemental analyses of α-ZnPc and β-ZnPc are satisfactory.

Table 1
Spectral parameters of α-ZnPc and β-ZnPc in DMSO, DMF and toluene.

	λ_Q (Abs)/nm (log ε)	λ_Q (Ems)/nm	$\Delta\lambda_{Stokes}$/nm	λ ($T_1 \rightarrow T_n$)/nm	E_S/eV
DMSO					
α-ZnPc	687 (5.07)	703	16	570	1.77
β-ZnPc	679 (4.48)	699	20	510	1.78
DMF					
α-ZnPc	685 (4.99)	702	17	560	1.77
β-ZnPc	676 (4.54)	694	18	490	1.79
Toluene					
α-ZnPc	690 (4.73)	711	21	550	1.75
β-ZnPc	676 (4.22)	692	16	510	1.80

3.2. Ground state electronic absorption spectra

The Q-band positions of α-ZnPc and β-ZnPc in DMF, DMSO and toluene are given in Table 1. The non-symmetric (splitting and broadening) nature of the Q-band of α-ZnPc (Figs. 1 and 2) is consistent with the non-planar distortion of the ZnPc ring by the substituents at the α-positions [35]. However, such spectral asymmetry was not observed for β-ZnPc (Fig. 1). It appears that steric hindrance arising from the quinoxalinyl substituents is more significant at the α-positions than at the β-positions. It is known that non-peripherally substituted MPc complexes are more liable to non-planar distortion than their peripherally substituted counterparts [35,36]. Also, the spectral asymmetry was observed only in

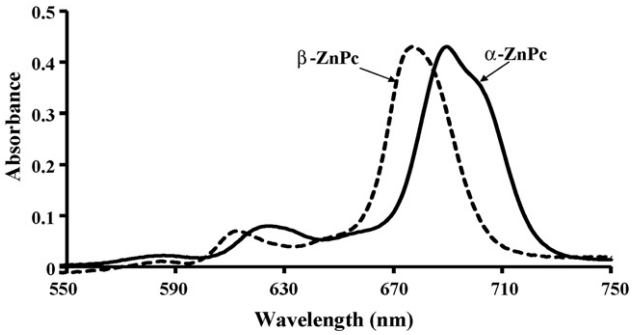

Fig. 1. UV–vis absorption spectra of α-ZnPc and β-ZnPc in toluene.

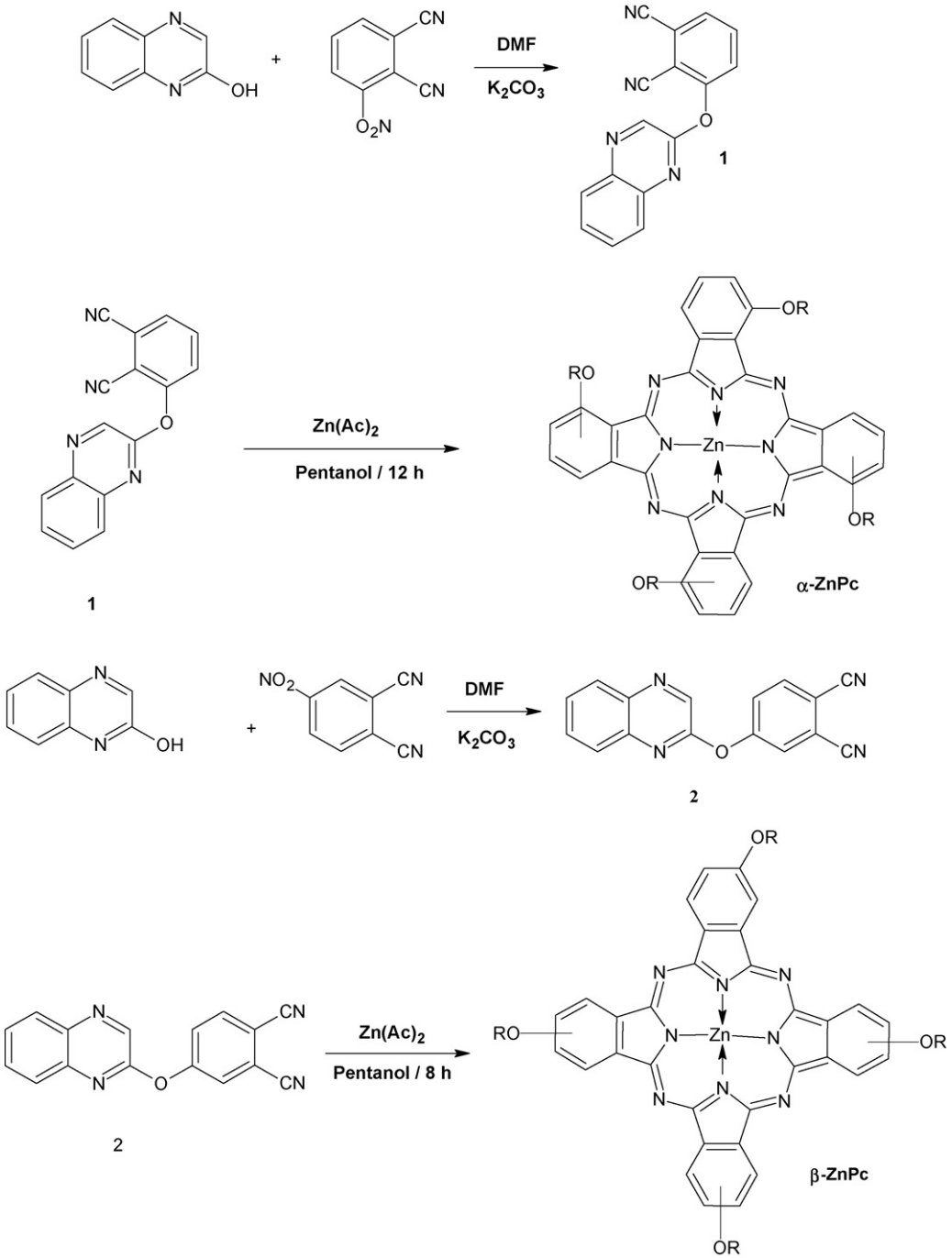

Scheme 1. Syntheses of α- and β-ZnPc.

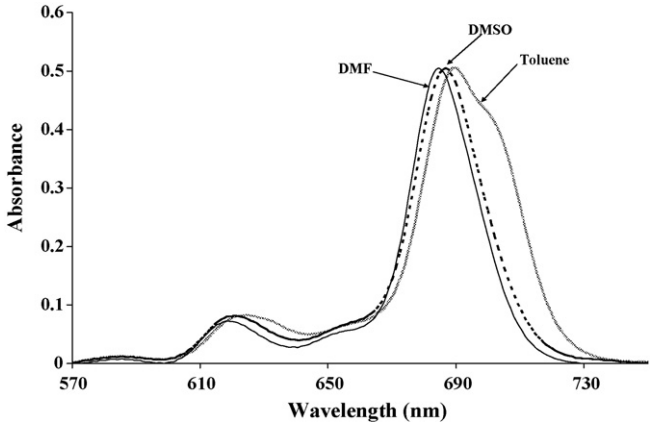

Fig. 2. UV–vis absorption spectra of α-ZnPc in DMF, DMSO and toulene.

toluene (a low-polarity solvent) and not in DMF and DMSO, which are polar solvents (Fig. 2), as observed before for ZnPc complexes bearing dendritic substituents at α-position [36]. One would have expected to observe the Q-band position at a longer wavelength in DMSO than toluene, on grounds of the higher refractive index of the former; however, the Q-band position in toluene is red-shifted relative to that in DMSO (Fig. 2), which is still attributed to non-planar distortion in toluene. The most notable result of macrocycle distortion is a bathochromic shift of the absorption spectrum, which is as a result of a destabilization of the π-system leading to a smaller HOMO–LUMO gap [37,38]. For β-ZnPc (in which distortion is not significant), the Q band position is observed at a shorter wavelength (676 nm) in toluene (and in DMF) than that in DMSO (679 nm), which is consistent with solvent refractive index considerations. In the three solvents, the Q-band positions of α-ZnPc are red-shifted relative to those of β-ZnPc, with the greatest red-shifting observed in toluene. Non-peripheral substitution greatly influences the energy levels of the molecular orbital and hence the absorption spectrum, whereas peripheral substitution has a smaller effect on the Q-band position. In α-ZnPc, the quinoxalinyl substituents are closer to the ring, hence they bring about greater destabilization of the a_{1u} orbital (HOMO), and result in larger bathochromic shifts. The greater red-shifting in toluene is as a result of the additional effect of the distortion of the macrocycle in this solvent, as discussed above.

3.3. Fluorescence spectra, lifetimes and quantum yields

The absorption and fluorescence excitation spectra of α-ZnPc (and of β-ZnPc) are similar in DMF, DMSO and toluene. Fig. 3 shows the fluorescence excitation and emission spectra of β-ZnPc in toluene. The Stokes' shifts range from 16 to 21 nm, which is

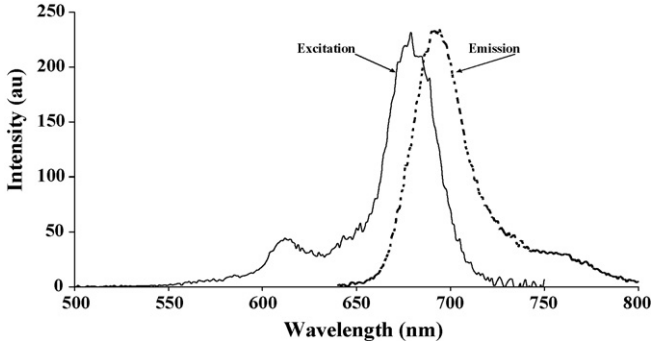

Fig. 3. Fluorescence excitation and emission spectra of β-ZnPc in toluene.

usual for ZnPc derivatives [27,39,40]. Fluorescence quantum yield (Φ_F) values for α-ZnPc and β-ZnPc in DMSO, DMF and toluene, are lower than those for unsubstituted ZnPc (Φ_F = 0.20, 0.17 and 0.07 in DMSO, DMF and toluene respectively [27]) (Table 2). This implies that the presence of quinoxalinyl substituents caused some fluorescence quenching of the parent ZnPc, and the extent of quenching is greater in α-ZnPc than in β-ZnPc. The lower Φ_F values for α-ZnPc (than for β-ZnPc) in the three solvents can be attributed to the proximity of the fluorescence-quenching substituents to the ZnPc ring. Φ_F is lower for α-ZnPc, in which the substituents are closer to the point of fusion to the ring. Comparing Φ_F values among the three solvent, the highest and lowest values were obtained in DMSO and toluene respectively. Φ_F values in the three solvents demonstrate that fluorescence is influenced by the environment of the fluorescing molecule, e.g., solvent parameters. Solvent effects on Φ_F are usually interpreted in terms of the Förster–Hoffman equation [41] (Eq. (7)), which predicts a direct dependence of Φ_F on solvent viscosity.

$$\text{Log}\,\Phi_F = C + x\,\text{log}\,\eta \tag{7}$$

The values of Φ_F in the three solvents are in conformity with the Förster–Hoffman equation. The viscosities of DMSO, DMF and toluene are 1.99, 0.78 and 0.59 cP respectively; the Φ_F values vary in the same order as solvent viscosities (Table 2).

3.4. Triplet quantum, yields and lifetimes

Triplet quantum yield (Φ_T) is the fraction of absorbing molecules that undergoes intersystem crossing to the metastable triplet excited state. Therefore, factors which induce spin–orbit coupling will certainly populate the triplet excited state. The effects of substituent position (α or β) and solvent on Φ_T values are shown in Table 2. α-ZnPc consistently exhibited higher Φ_T values than β-ZnPc in the three solvents. Any feature that promotes structural distortion will enhance intersystem crossing to the triplet excited state [36,42]. As stated earlier, α-substitution supports molecular distortion, hence higher values of Φ_T for α-ZnPc (than for β-ZnPc) are expected, as shown in Table 2. In this vein, the particularly high Φ_T value of α-ZnPc in toluene (0.71) could be attributed to non-planar distortion of the complex in this solvent. There is no well defined trend in the variation of Φ_T with solvent type; however, the values are slightly higher in DMSO than in DMF. Triplet lifetimes (τ_T) of the complexes are listed in Table 2. The values are longer for α-ZnPc than for β-ZnPc. Among the three solvents, the order of τ_T is DMSO > DMF > toluene. The reason for the large difference in value (going from DMSO to DMF and toluene) is not clear, but could partly be ascribed to the higher viscosity of DMSO (1.99 cP) than those of DMF (0.78 cP) and toluene(0.59 cP). The rate of non-radiative deactivation and molecular motion are expected to be decreased in a viscous solvent like DMSO, and be increased in toluene, having a low viscosity. The triplet states of both α-ZnPc and β-ZnPc in the three solvents follow a mono-exponential decay profile; the triplet decay profile for α-ZnPc in DMSO is shown in Fig. 4.

Quantum yields of internal conversion (Φ_{IC}) do not differ much as the solvent is changed, which implies that the quantum yields of the other two deactivation processes (Φ_F and Φ_T) are complimentary to each other. Φ_{IC} values are somewhat higher in β-ZnPc.

3.5. Singlet oxygen and photodegradation quantum yields

Singlet oxygen is the lowest excited state of the oxygen molecule. Singlet oxygen is generated in solution by photosensitization. A photosensitizer is irradiated to its singlet excited state, followed by intersystem crossing to its triplet excited state. The triplet may then produce singlet oxygen (Type II process) via energy transfer to

Table 2
Photophysical and photochemical properties of α-ZnPc and β-ZnPc in DMSO, DMF and toluene.

	τ_T/μs[a]	Φ_F	Φ_T	Φ_{IC}	Φ_Δ	$10^5\Phi_{Pd}$	$10^{-4}k_T$ (k_{obs})/s^{-1}	$10^{-4}k_{T(O)}$/s^{-1}[a]	$10^{-8}k_b$/M^{-1} s^{-1}[b]
DMSO									
α-ZnPc	160 (100)	0.13	0.62	0.25	0.57	2.35	0.62 (1.00)	0.38	0.13
β-ZnPc	125 (90)	0.17	0.53	0.30	0.51	1.89	0.80 (1.11)	0.31	0.11
DMF									
α-ZnPc	7.8 (4.1)	0.10	0.57	0.33	0.51	1.04	12.82 (24.39)	11.57	4.13
β-ZnPc	4.2 (3.1)	0.14	0.51	0.35	0.47	1.73	23.81 (32.26)	8.45	3.02
Toluene									
α-ZnPc	7.0 (3.3)	0.03	0.71	0.26	0.55	0.71	14.29 (30.30)	16.02	5.72
β-ZnPc	5.1 (3.0)	0.06	0.55	0.39	0.49	0.98	19.61 (33.33)	13.73	4.90

[a] Values in brackets for air-saturated solutions (in the presence of oxygen).
[b] Calculated using Eq. (9) and taking $[O_2]$ to be 2.8×10^{-4} M [45].

triplet ground state oxygen. This mechanism suggests that the efficiency of singlet oxygen generation (measured as singlet oxygen quantum yield, Φ_Δ), should depend on the energy (E_T), quantum yield (Φ_T) and lifetime (τ_T) of the triplet state, among other factors. As in the case of Φ_T values, Φ_Δ values are larger for α-ZnPc than for β-ZnPc in the three solvents. The values are also consistent with the τ_T values as expected. Solvent effects on Φ_Δ values are not well pronounced, but slightly lower values were obtained in DMF and toluene. Considering, the huge discrepancy between τ_T values obtained in DMSO and those obtained in DMF and toluene, one would expect a concomitant large difference between Φ_Δ values in DMSO and those in DMF and toluene. However, the values, though lower in DMF and toluene, are still long enough for appreciable sensitization of singlet oxygen production. This observation suggests that the differences in τ_T values in the various solvents, do not significantly affect Φ_Δ values. Photodegradation values were within the values typical of stable MPc complexes [40].

3.6. Kinetics of interaction of triplet states with triplet oxygen

The triplet lifetimes of the complexes decreased in the presence ambient oxygen, compared to those obtained in argon-saturated solutions (Fig. 5). This observation is expected because triplet oxygen is known [42,43] to be an excellent quencher of the triplet excited states of MPc-based photosensitizers, forming singlet oxygen as discussed above. The lifetimes and decay rate constants of α-ZnPc and β-ZnPc in the presence and absence of oxygen (and in three different solvents) are shown in Table 2. The rate constants for spontaneous triplet decay were calculated as the reciprocals of the respective triplet lifetimes in deaerated (argon-saturated) solutions ($k_T = 1/\tau_T$); while the decay rate constants in the presence of oxygen were calculated as the reciprocals of the observed triplet lifetimes in the presence of oxygen ($k_{T(obs)} = 1/\tau_{T(obs)}$). It should however be noted that $k_{T(obs)}$ has two components, as given by Eq. (8):

$$k_{T(obs)} = k_T + k_{T(O)} \tag{8}$$

where $k_{T(O)}$ is the pseudo-first order rate constant for the quenching of the triplet state by oxygen (as oxygen is in excess over the MPc triplet state), and is defined by Eq. (9):

$$k_{T(O)} = k_b[O_2] \tag{9}$$

where k_b is the bimolecular rate constant and $[O_2]$, concentration of oxygen in air-saturated solution, taken as 2.8×10^{-4} M [44].

Values of k_T, $k_{T(obs)}$, $k_{T(O)}$ and k_b are given in Table 2. In the three solvents, k_T and k_{obs} are lower for α-ZnPc than for β-ZnPc, as expected on grounds of longer τ_T of the former. However, α-ZnPc exhibits higher values of $k_{T(O)}$ and k_b than β-ZnPc, which implies that quinoxalinyl substituents on α-positions make the ZnPc ring more vulnerable to oxygen quenching than when they are on β-positions. The values of k_b are smaller than the diffusion-controlled values ($\sim 10^{10}$ M^{-1} s^{-1} [45]), which could have resulted from steric shielding of the triplet states or low quenching efficiencies in the complexes [46]. The fact that k_b values are smaller for β-ZnPc suggests that these molecules are more sterically shielded from the diffusing oxygen molecules than α-ZnPc molecules. Solvent effect on the rate constant values is well pronounced, with the values being consistently smaller in the most viscous of the solvent (DMSO). The small values of k_T in DMSO are ascribed to greater hindrance to non-radiative deactivation, molecular rotation and translation in this solvent. Again, the diffusion coefficient of oxygen is the three solvents is in the order DMSO > DMF > toluene; the rate of collision of oxygen molecules with the triplet state is lower in DMSO than in DMF and toluene, hence smaller values of $k_{T(O)}$ and k_b in DMSO are not unexpected.

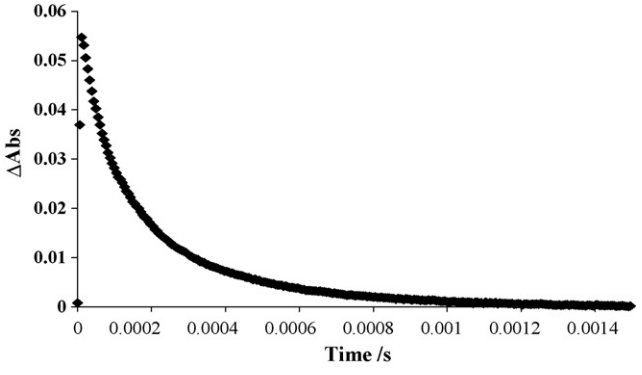

Fig. 4. Mono-exponential triplet decay profile for α-ZnPc in DMSO.

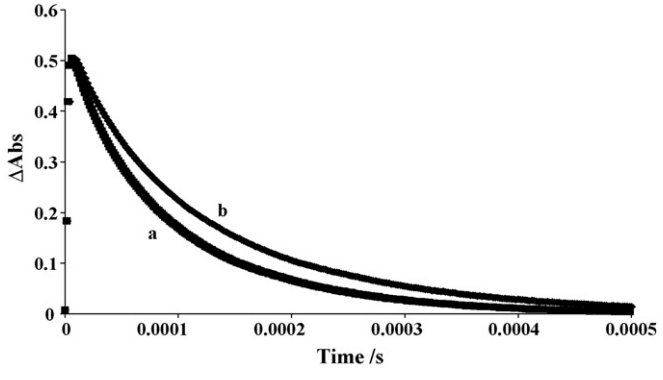

Fig. 5. Triplet decay profiles for β-ZnPc in DMSO (a) in the absence of oxygen and (b) in the presence of oxygen.

3.7. Conclusion

This work has described the syntheses, spectral and photophysicochemical properties of *tetra*(quinoxalinyl)phthalocyaninato zinc(II), in which the substituents are at the non-peripheral (α-ZnPc) and peripheral (β-ZnPc) positions respectively. The syntheses of the complexes were confirmed by IR and NMR spectroscopies, as well as elemental analysis. It has been revealed that the presence of the quinoxalinyl substituents on ring α-positions brought about greater distortions to the parent MPc ring than they do on β-positions, as evident from the greater bathochromic shift in the absorption wavelength of the former than that of the latter. Such distortions are more severe in low-polarity solvent–toluene than in DMSO and DMF, contrary to what might be expected on the grounds of the solvents' refractive indices consideration. Both complexes are less fluorescent than the unsubstituted ZnPc, suggesting the fluorescence quenching effect exerted by the quinoxalinyl substituents on the parent ZnPc. α-ZnPc is not as fluorescent as β-ZnPc, but exhibits greater triplet yields; these observations were again attributed to the greater non-planar distortion in the former. However, singlet oxygen quantum yields were comparable for both complexes, though α-ZnPc exhibited slightly higher values. Φ_F values were observed to vary with solvent refractive index, in conformity with Förster–Hoffman relation. Triplet state quenching by oxygen was more effective in α-ZnPc than in β-ZnPc, judging from the respective values of bimolecular rate constants for the quenching processes. Such triplet state quenching was found to be most effective in the least viscous solvent–toluene, due to the higher diffusivity of oxygen in this solvent.

References

[1] M. Ebadi, C. Alexiou, A.B.P. Lever, Can. J. Chem. 7 (2001) 992–1001.
[2] K. De Wael, A. Adriaens, Talanta 74 (2008) 1562–1567.
[3] P. Kluson, M. Drobek, T. Strasak, J. Krysa, M. Karaskova, J. Rakusan, J. Mol. Cat. A: Chem. 272 (2007) 213–219.
[4] K.T. Ranjit, I. Willner, J. Phys. Chem. B 102 (1998) 9397–9403.
[5] E.M. Maya, A.W. Snow, J.S. Shirk, R.G. Pong, S.R. Flom, G.L. Roberts, J. Mater. Chem. 13 (2003) 1603–1613.
[6] N.S. Nalwa, J.S. Shirk, in: A.P.B. Lever, C.C. Leznoff (Eds.), Phthalocyanines: Properties and Applications, vol. 4, Willey–VCH, New York, 1996 (Chapter 3).
[7] S. Radhakrishnann, S.D. Deshpande, Sensors 2 (2002) 185–194.
[8] J. Oni, P. Westbroek, T. Nyokong, Electroanalysis 14 (2002) 1165–1168.
[9] D. Wöhrle, L. Kreienhoop, D. Schlettwein, in: A.P.B. Lever, C.C. Leznoff (Eds.), Phthalocyanines: Properties and Applications, vol. 4, Willey–VCH, New York, 1996 (Chapter 3).
[10] I. Rosenthal, Photochem. Photobiol. 53 (1991) 859–870.
[11] J.D. Spikes, J. Photochem. Photobiol. B: Biol. 6 (1990) 259–274.
[12] J.D. Spikes, Photochem. Photobiol. 43 (1986) 691–699.
[13] S.G. Bown, C.J. Tralau, P.D.S. Colendge, D.T. Akdemir, T.J. Wieman, Br. J. Cancer 54 (1987) 43–52.
[14] S.B. Brown, T.G. Truscott, Chem. Br. (1993) 955–958.
[15] R. Bonnett, Chemical Aspects of Photodynamic Therapy, Gordon and Breach Science, Canada, 2000.
[16] M. Fournier, P. Claude, D. Houde, R. Ouellet, J.E. van Lier, Photochem. Photobiol. Sci. 3 (2004) 120–126.
[17] J.-P. Daziano, S. Steenken, C. Chabannon, P. Mannoni, M. Chanon, M. Julliard, Photochem. Photobiol. 64 (2008) 712–719.
[18] S. Fery-Forgues, D. Lavabre, J. Chem. Ed. 76 (1999) 1260–1264.
[19] J. Fu, X.Y. Li, D.K.P. Ng, C. Wu, Langmuir 18 (2002) 3843–3847.
[20] A. Montalban, H. Meunier, R. Ostler, A. Barrett, B. Hoffman, G. Rumbles, J. Phys. Chem. A 103 (1999) 4352–4358.
[21] P. Kubát, J. Mosinger, J. Photochem. Photobiol. A: Chem. 96 (1996) 93–97.
[22] T.H. Tran-Thi, C. Desforge, C.C. Thiec, J. Phys. Chem. 93 (1989) 1226–1233.
[23] J. Kossanyi, D. Chahraoui, Int. J. Photoenergy 2 (2000) 9–14.
[24] S.M. Bishop, A. Beeby, A.W. Parker, M.S.C. Foley, D. Phillips, J. Photochem. Photobiol. A: Chem. 90 (1995) 39–44.
[25] N. Kuznetsova, N. Gretsova, E. Kalmykova, E. Makarova, S. Dashkevich, V. Negrimovskii, O. Kaliya, E. Luk'yanets, Russ. J. Gen. Chem. 70 (2000) 133–140.
[26] W. Spiller, H. Kliesch, D. Wohrle, S. Hackbarth, B. Roder, G. Schnurpfeil, J. Porphyrins Phthalocyanines 2 (1998) 145–158.
[27] A. Ogunsipe, D. Maree, T. Nyokong, J. Mol. Struct. 650 (2003) 131–140.
[28] I. Gürol, V. Ahsen, J. Porphyrins Phthalocyanines 4 (2000) 620–626.
[29] A.W. Snow, J.S. Shirk, R.G.S. Pong, J. Porphyrins Phthalocyanines 4 (2000) 518.
[30] S.E. Maree, T. Nyokong, J. Porphyrins Phthalocyanines 5 (2001) 782–792.
[31] M.S. Ağırtaş, Inorg. Chem. Acta 360 (2007) 2499–2502.
[32] S. Dabak, G. Gümüş, A. Gül, Ö. Bekaroğlu, J. Coord. Chem. 38 (2001) 287–293.
[33] M.M. El-Nahass, K.F. Abd-El-Rahman, A.A.A. Darwish, Mater. Chem. Phys. 92 (2005) 185.
[34] S. Marcuccio, P.I. Svirskaya, S. Greenberg, A.B.P. Lever, Can. J. Chem. 63 (1985) 3057.
[35] N. Kobayashi, T. Fukuda, K. Ueno, H. Ogino, J. Am. Chem. Soc. 123 (2001) 10740–10741.
[36] K. Kasuga, N. Matsuura, K. Inoue, M. Handa, T. Sugimori, K. Isa, M. Nakata, Chem. Lett. (2002) 352–356.
[37] M.O. Senge, Chem. Commun. (2006) 243–256.
[38] K.M. Barkigia, L. Chantranupong, K.M. Smith, J. Fajer, J. Am. Chem. Soc. 110 (1988) 7566–7567.
[39] M.O. Senge, M.W. Renner, W.W. Kalisch, J. Fajer, J. Chem. Soc., Dalton Trans. (2000) 381–386.
[40] A. Ogunsipe, J.-Y. Chen, T. Nyokong, New J. Chem. 28 (2004) 822–827.
[41] T. Förster, G. Hoffmann, Z. Phys. Chem. 75 (1971) 63–76.
[42] J.-H. Ha, G.Y. Jung, M.-S. Kim, Y.H. Lee, K. Shin, Y.-R. Kim, Bull. Korean Chem. Soc. 22 (2001) 63–67.
[43] S. Foley, G. Jones, R. Liuzzi, D.J. McGarvey, M.H. Perry, T.G. Truscott, J. Chem. Soc., Perkin Trans. 2 (1997) 1725–1730.
[44] R. Battino (Ed.), Solubility Data Series, vol. 7, Pergamon Press, Oxford, 1981, p. 2.
[45] S.L. Murov, I. Carmichael, G.L. Hug, Handbook of Photochemistry, 2nd edition, M. Decker, New York, 1993, pp. 207.
[46] J.R. Lakowicz, Pronciples of Fluorescence Spectroscopy, 2nd edition, Kluwer Academic/Plenum Publishers, New York, 1999, pp. 281.